AIAA JOURNAL
Vol. 40, No. 8, August 2002

Effect of Surface Roughness on Unseparated Shock-Wave/ Turbulent Boundary-Layer Interactions

H. Babinsky*
University of Cambridge, Cambridge, England CB2 1PZ, United Kingdom
and
G. R. Inger†
Iowa State University, Ames, Iowa 50011-3231

The effect of surface roughness and step changes of surface roughness on an unseparated incipient shock-wave/turbulent boundary-layer interaction has been studied using complementary experimental and theoretical investigations. It was found that step changes in surface roughness lead to nonequilibrium boundary layers displaying different characteristics in the near-wall and far-wall regions. Both theory and experiment confirmed that the dominant effect of roughness, even in configurations featuring step changes of surface properties, is a change of boundary-layer displacement thickness and that the upstream influence of the interaction scales very well with the roughness modified incoming displacement thickness in all cases. The theory also identified small additional roughness effects, particularly for configurations featuring a smooth/rough wall transition ahead of the interaction.

Nomenclature

B	=	roughness-dependent constant in Eq. (1)
C_f	=	skin-friction coefficient
$C_{p,\mathrm{is}}$	=	pressure coefficient at incipient separation
C_1, C_2	=	constants defined following Eq. (5)
H	=	boundary-layer shape factor, δ^*/θ^*
h	=	roughness height
l_u	=	upstream influence distance
M	=	Mach number
N	=	power law exponent
T	=	temperature
U	=	velocity in x direction
U_τ	=	skin-friction velocity, $(\tau_w/\rho_W)^{1/2}$
U^+	=	U in law of the wall variables, U/U_τ
W	=	Cole's wake function
x	=	streamwise coordinate
y	=	vertical coordinate
y^+	=	law of the wall coordinate, $y\,U_\tau/\nu_W$
β	=	$\sqrt{(M_e^2 - 1)}$
δ	=	boundary-layer thickness
δ^*	=	displacement thickness
η	=	integration variable
θ^*	=	momentum thickness
κ	=	law of the wall constant
ν	=	kinematic viscosity
ρ	=	density
τ	=	shear stress

Subscripts

e	=	boundary-layer edge conditions
i	=	inner deck
LSL	=	laminar sublayer
R	=	rough surface conditions
S	=	smooth surface conditions
w	=	wall conditions
0	=	upstream conditions
∞	=	freestream conditions

Received 18 August 2000; revision received 5 November 2001; accepted for publication 15 February 2002.

*Senior Lecturer in Aerodynamics, Engineering Department, Trumpington Street. Member AIAA.

†Professor, Aerospace Engineering and Engineering Mechanics. Associate Fellow AIAA.

Introduction

In many supersonic flows of practical importance, the interaction of a shock wave with a boundary layer plays a critical role. Shock wave/boundary layer interactions (SWBIs) not only significantly influence local features, but they can also strongly affect the global flow by causing separation or by changing boundary-layer characteristics for a large distance downstream. Although this phenomenon has been researched widely for many decades, the effect of surface roughness has been the subject of relatively few studies. However, the effects of roughness are significant in many practical applications, especially at large Reynolds numbers where the length scales within the boundary layer are particularly small. Such roughness effects would be associated, for example, with the mesh of porous wall sections for boundary-layer control by suction, or with overall distributed surface grittiness.

The effect of surface roughness placed underneath a hypersonic compression corner was investigated by Disimile and Scaggs,[1] who found that roughness was capable of significantly enlarging flow separation in cases where the equivalent smooth wall flow appeared to be attached. Similar results are reported by Holden[2] and Inger[3] for a variety of supersonic and hypersonic flow configurations, thus emphasizing that roughness can significantly alter the character of a shock/boundary-layer interaction. In contrast, a study by Babinsky and Edwards,[4] which investigated the influence of a region of roughness upstream of an interaction, found that, although the effects of roughness on the boundary layer profile persisted far downstream, the shock/boundary-layer interaction itself was only marginally affected. It is thought that triple-deck theory can provide insight into the physical mechanisms of rough wall shock/boundary-layer interactions and lead to an understanding of roughness effects. A first combined theoretical and experimental investigation into this problem by Inger and Gendt[5] has identified some of the significant factors; however, in its nature, this was only a pilot study and further, more detailed, measurements are needed. More recently, Babinsky et al.[6] presented an initial experimental/theoretical study into rough wall interactions with particular emphasis on cases where the upstream boundary layer was subject to step changes in roughness (rough to smooth and smooth to rough). The work presented here is a continuation of this study.

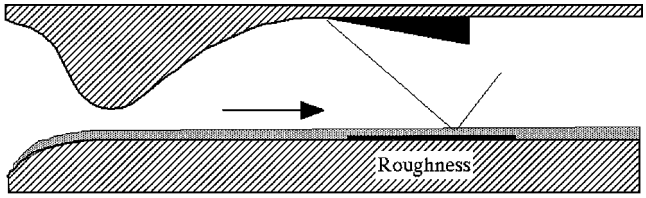

Fig. 1 Experimental configuration.

To study the effects of surface roughness on a shock/boundary-layer interaction, the incipient shock configuration seen in Fig. 1 was chosen. In particular, the length of the interaction on the surface is examined because it is an easily quantified feature that is thought to be sensitive to changes in the interaction physics. Previous research on such impinging shock interactions by Délery[7] has shown that, for a given shape factor of the oncoming boundary layer, surface pressure distributions collapse for a large variety of shock strengths and Reynolds numbers when scaled with incoming boundary-layer thickness. He concluded that the most important parameters governing interaction length are boundary-layer shape factor and thickness.

The effect of roughness, or blowing and suction, is, therefore, understood to change the interaction through its effects on the boundary-layer profile entering the interaction region. Because roughness and blowing increase boundary-layer thickness and shape factor, a subsequent increase in interaction length is expected. An investigation by Squire and Smith[8] has shown this to be essentially correct for boundary layers modified by blowing. Furthermore, these authors could not find any scaling between interaction length and incoming boundary-layer thickness and suggested using the distance of the sonic line from the wall downstream of the interaction as a scaling parameter. Somewhat surprisingly, their study also indicated that the shock strength required for incipient separation was independent of the level of blowing. One possible explanation for this behavior is that an increased boundary-layer thickness automatically leads to an increased smearing of the shock-induced pressure rise, which in turn makes separation less likely. On the other hand, blowing (or roughness) also changes the shape and fullness of the incoming boundary layer that is working toward an earlier separation onset.

The aim of the current research is to perform a similar study on the effects of roughness and in particular include the influence of surface changes between rough and smooth at locations close to the interaction. Boundary layers in the vicinity of such changes are believed to be perturbed from equilibrium, and this may supply some insight toward the correct scaling quantities. In parallel, triple-deck theory is used to suggest scaling laws based on a theoretical derivation. It is also hoped that this study may help to understand the importance of both thickness and shape changes in an incoming boundary layer on the physics of a shock/boundary-layer interaction.

Theoretical Analysis

Our theoretical study particularly focuses on small ($h/\delta \ll 1$) distributed subboundary-layer roughness of the classical sand grain type that falls under the law of the wall/law of the wake framework. Such roughness when existing upstream of the SBLI zone will alter both the thickness and the shape of the incoming boundary-layer profile on which the subsequent interaction depends. Furthermore the presence of roughness in the SBLI zone itself will affect the triple-deck structure of the interaction disturbance field, especially its inner layer; indeed, at higher Reynolds numbers even moderate roughness may obliterate the inner deck altogether.

Incoming Boundary Layer

Within the law of the wall/law of the wake concept adopted here, the incoming velocity profile is described by the well-known expression (e.g., White[9])

$$U_0^+(y^+) \equiv \left[U_0(y^+)/U_\tau\right] = B + (1/\kappa)\ell n y^+ + (1/\kappa)W(y/\delta_0) \quad (1)$$

Here, $U_\tau^2 \equiv \tau_w/\rho_w$, W is Cole's wake function, and B contains the roughness-induced downward shift of the inner logarithmic region that depends on the nondimensional roughness parameter $h^+ \equiv U_\tau h/\nu_w$ as given in the literature.[9] For the purposes of the present study at moderate Mach numbers, it is assumed sufficient to base properties on wall values instead of using a more complicated compressibility transformation version of Eq. (1).

In accordance with this model, the main physical effects of roughness fall into three regimes. The first regime is the so-called hydraulically smooth regime, $h \le y_{LSL}(h^+ \le 7\text{–}12)$, where the roughness is buried within the laminar (linear) sublayer and so has no sensible effect on the flow. The second regime is an intermediate, above-critical regime $7 \le h^+ \le 70$, in which the roughness begins to have discernible effects on the flow in that it shifts $U^+(y^+)$ downward, thickens the boundary layer, and introduces a drag increase that reduces the velocity in the physical $U(y)$ profile. This is shown schematically in Fig. 2. The last-mentioned feature can be approximately modeled by the well-known power law expression

$$U/U_e \approx (y/\delta)^N \quad (2)$$

where $N \approx \frac{1}{7}$ for smooth surfaces but $\approx \frac{1}{5}$–$\frac{1}{4}$ for rough ones. The third regime is the fully rough case $h^+ > 70$ (but $h < \delta$), where the turbulent stirring effect of roughness is so big that it obliterates all vestiges of the laminar sublayer and imposes its own scale on the law of the wall region. For this regime, it is known that B takes the limiting value $B \approx B_R(h^+) - 1/\kappa\,\ell n h^+$ and, hence, produces the viscosity independent law of the wall profile:

$$U^+ = B_R + (1/\kappa)\ell n(y/h) + (\pi/\kappa)W \quad (3)$$

where $B_R = 8\text{–}9$ depends on the roughness geometry and density. Because of its database, Eq. (3) applies only above the maximum roughness crests.

Interaction Region

A second element of our theoretical approach is the triple-deck concept for the disturbance flow structure in the SBLI zone; a schematic of this is given in Fig. 3 for a smooth wall. This is used as the foundation for a theory of how roughness affects the interaction physics. The present theory addresses the fully rough case,

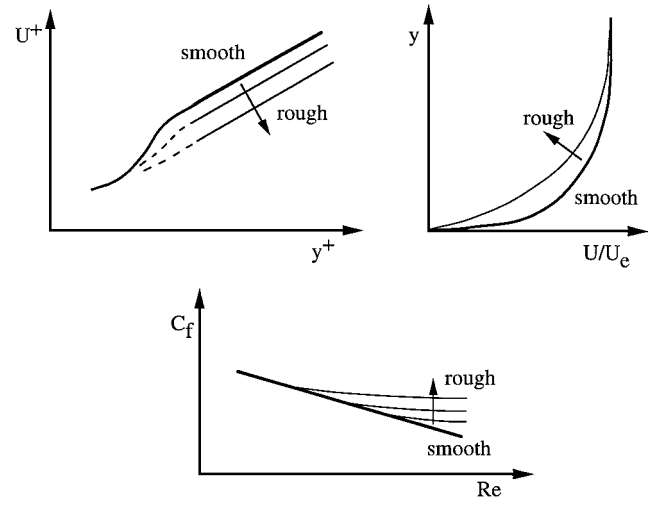

Intermediate roughness regime $11 \le h^+ \le 70$

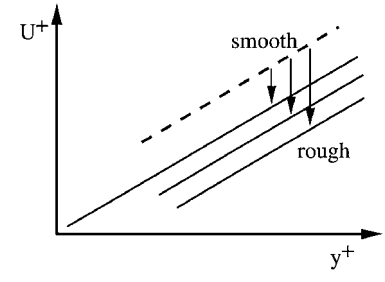

Fully rough regime $h^+ > 70$

Fig. 2 Physical effects of roughness on the incoming turbulent boundary layer ($h/\delta < 1$): schematic.

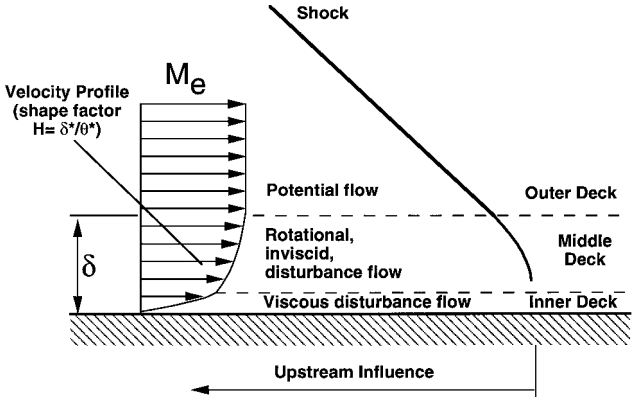

Fig. 3 Triple-deck model of shock/boundary-layer interaction.

which by analogy with its aforementioned effect on the laminar sublayer would be expected to also wipe out the inner portion of the interactive triple-deck structure.

The analysis consists of an extension of a very successful triple-deck perturbation theory[10] originally developed for smooth surfaces, which accounts for nonvanishing eddy viscosity and slip velocity near the wall when roughness is present in the SBLI zone (Fig. 3). When purely supersonic external flow and nonseparating incident shock strengths are assumed, the resulting Fourier transform method inviscid disturbance flow analysis for the rotational middle deck for arbitrary incoming boundary-layer profiles (now including possible upstream roughness) yields the upstream ($x < 0$) pressure rise $p' \approx \Delta_p \exp(-x/l_u)$, where Δ_p is the incident shock strength and l_u is the characteristic upstream influence distance given by[11]

$$\beta \frac{l_u}{\delta_0} \approx M_e^2 \int_{y_i/\delta_0}^{1} \left[\frac{1 - M_0^2(\eta)}{M_0^2(\eta)} \right] \mathrm{d}\eta + \left(\frac{\beta}{M_e} \right)^2 \int_{y_i/\delta_0}^{1} M_0^2(\eta)\, \mathrm{d}\eta \quad (4)$$

The lower limit y_i is the effective displacement thickness of the underlying inner deck, which for SBLI zone roughness higher than the inner deck (often the case in practice) should be replaced by the average sand-grain roughness height h with a nonzero slip Mach number $M_0(y_i) = M_0(h)$. In what follows, we focus on the upstream influence property because it is an important experimental feature of the interactive pressure distribution.

Equation (4) indicates that the upstream influence derives from two sources: 1) a Reynolds number-independent contribution from the profile shape across the middle deck and 2) a Reynolds number-dependent contribution from the region adjacent to the wall. Numerically, both contributions have been shown[3] to be of order unity, consistent with the experimental observation that $l_u \approx \delta_0$ for turbulent interactions.[12] The general relationship [Eq. (4)] may now be developed into a more revealing prediction by breaking the integration range down into an inner law of the wall range $h^+ \le y^+ \le 250$ (for example) where the wake component of Eq. (1) is negligible and an outer defect range $250 \le y^+ \le U_\tau \delta_0/\nu_w$ and $U_0^+ \ge 19$ where a power law Mach number profile $M_0 \approx M_e(y/\delta_0)^N$ akin to Eq. (2) is a reasonable approximation. Then when Eq. (1) in the form $y^+ = \exp(-\kappa B)\exp(\kappa U_0^+)$ is used and the speed of sound is based on wall conditions when evaluating the dominant inner law of the wall contributions, Eq. (4) can be shown to yield the following closed-form result:

$$\beta \frac{l_u}{\delta_0^*} \approx C_1 \left[\frac{e^{\kappa B}}{U_{0w}^+} + C_2 \right] + \frac{4(1+N)}{1-4N^2} \left[1 - \frac{1-2N}{2} M_e^2 \right] + \frac{y_i}{\delta_0^*} \quad (5)$$

where

$$C_1 \equiv \frac{\kappa e^{W(1)} \sqrt{T_e/T_w}}{(1+\pi)(C_f/2)^{\frac{3}{2}} \exp\left[\kappa \sqrt{2(T_e/T_w)/C_f} \right]}$$

$$C_2 \equiv \left[\exp\left(\kappa U_0^+\right) \Big/ U_0^{+^2} \right]_{U_0^+ = 19}$$

have been derived using the law of the wall/wake relationships[9]

$$U_\tau \delta_0/\nu_w = \exp[\kappa U_e/U_\tau - \kappa B - W(1)]$$

$$\delta_0^*/\delta = (N/1+N) \approx (1+\pi) U_\tau/\kappa U_e$$

$$U_\tau/U_e = \sqrt{(T_W/T_e)(C_f/2)}$$

Note that we have rescaled l_u in terms of δ_0^* instead of δ_0; the reason for this will appear shortly. Also note that the dominant constant C_1 in Eq. (5) is virtually independent of the boundary-layer thickness (whether rough or smooth wall) and changes only slightly with roughness effect on C_f because the separate effects on the $C_f^{3/2}$ and exponential terms in C_1 are opposite and nearly cancel out.

In applying Eq. (5), we may now distinguish three different cases of roughness placement. In the case of completely smooth surface throughout, Eq. (5) yields

$$\left(\beta \frac{l_u}{\delta_0^*} \right)_S \approx C_{1,S} \left[\frac{e^{\kappa B_S}}{U_{0w}^+(y_i^+)} + C_2 \right] + \frac{4(1+N_S)}{1-4N_S^2} \left[1 - \frac{1-2N_S}{2} M_e^2 \right] \quad (6)$$

The last term in Eq. (5) has been dropped as negligible compared to the C_1 term, and the value of y_i is the inner-deck thickness given by the turbulent interaction theory of Inger[10] with $U_{0,w}^+ \approx y_{i,w}^+ \equiv U_\tau y_i/\nu_w$ for $y_i^+ \le 7$, and $U_{0,w}^+ \approx B_S + 2.5 \ln y_i^+$ otherwise.

In the second case, where the upstream region is smooth but a patch of fully rough, inner deck-destroying roughness occupies the SBLI region, we have instead that $y_i \approx h$ with the laminar sublayer term $\propto e^{\kappa B}/U_{0,w}^+$ dropped in Eq. (5) resulting in the prediction that

$$\left(\beta \frac{l_u}{\delta_0^*} \right)_{\substack{\text{rough SBLI} \\ \text{zone only}}} \approx C_{1,S} C_2 + \frac{4(1+N_S)}{1-4N_S^2} \left[1 - \frac{1-2N_S}{2} M_e^2 \right] + \frac{h}{\delta_{0,S}^*} \quad (7)$$

where the last term here is a minor contribution. The SBLI zone here is effectively a double-decked rotational inviscid flow with a slip velocity at the bottom.

Finally in the third case of a fully roughened surface throughout, where the incoming boundary layer is also influenced by the roughness, we get

$$\left(\beta \frac{l_u}{\delta_0^*} \right)_R \approx C_{1,R} C_2 + \frac{4(1+N_R)}{1-4N_R^2} \left[1 - \frac{1-2N_R}{2} M_e^2 \right] + \frac{h}{\delta_{0,R}^*} \quad (8)$$

When it is kept in mind that $h/\delta_0^* \ll 1$, that C_1 is virtually independent of boundary-layer thickness and only weakly dependent on roughness (see foregoing text), and that N is related to the incoming boundary layer shape factor H by $N \approx (H-1)/2$, comparison of these three results [Eqs. (6–8)] yields some important predictions for the upstream region of nonseparating interactions.

First, the dominant effect of roughness is simply its effect on the incoming boundary-layer displacement thickness: When l_u is scaled with respect to the appropriate δ_0^*, the residual effects of roughness are rather small. This is in fact strikingly confirmed by the present experiments, as will be shown. The idea of scaling streamwise distance with displacement thickness was first suggested by Gadd (e.g., see Gadd et al.[13]) for smooth wall surfaces. Here, this idea is derived theoretically, and it is predicted to be also valid for rough surfaces.

Second, the shape of the incoming boundary-layer profile, as regards the presence of upstream roughness, has only a minor effect on the upstream influence.

Third, the direct effect of the roughness height itself on l_u is a rather weak one. Note, however, that this does not hold in the immediate vicinity and downstream of the shock front.

The foregoing can be carried further into an estimate of the roughness effect on incipient separation as well. From a Chapman-type order of magnitude analysis of the turbulent interaction problem, it can be shown that the interaction pressure coefficient needed to first produce $C_f \approx 0$ locally in the SBLI zone is of the order

$$C_{p,\mathrm{is}} \approx \left[\beta \frac{l_u}{\delta_0}\right]^{-1} = \frac{[\beta l_u/\delta_0^*]^{-1}}{\delta_0^*/\delta_0} \approx \frac{[\beta l_u/\delta_0^*]^{-1}}{\sqrt{C_{f,0}}} \tag{9}$$

where $C_{f,0}$ is the undisturbed skin friction upstream.

Because we have just shown that the numerator of Eq. (9) is virtually independent of roughness, Eq. (9) predicts that the increased skin friction would correspondingly reduce $C_{p,\mathrm{is}}$ and, thus, hasten the onset of separation.

Experimental Setup

Figure 1 shows the experimental arrangement. The high-speed wind tunnel of the Department of Engineering at Cambridge University is fitted with half-liners to allow a turbulent boundary layer to grow along the working section floor (width, of 0.11 m) at a flow Mach number of 2.5. The reservoir total pressure is 370 kPa and the Reynolds number per unit meter is in the range of 40×10^6. The smooth surface boundary-layer thickness is of the order of 6 mm at the interaction location. A full-span wedge placed at variable angles onto the ceiling of the wind tunnel generates an oblique shock wave impinging on the floor boundary layer. The wedge is of sufficient length to prevent the trailing-edge expansion fan from influencing the interaction. The wedge angles used were 6 and 7 deg, giving shock strengths just below incipient separation. Three types of sand-grain roughness were investigated, P1200, P400, and P150, having roughness heights of $h^+ = 4.3$, 9.9, and 28.2, respectively (based on smooth wall boundary-layer parameters). For the Mach number of the present experiments ($M_\infty = 2.5$), the two smaller roughnesses lie below the sonic line of the smooth wall boundary layer, whereas the peak dimension of the largest is comparable to the smooth surface sonic height.

As shown in Fig. 4, roughness elements were placed in a variety of locations along the surface to examine the effects of roughness, underneath the interaction as well as upstream, and sudden changes of surface properties. Cases are numbered from 0 (no roughness) to 7 (roughness throughout) in order of increasing amount of roughness upstream of the interaction location.

Surface pressures were measured using pressure tappings along the centerline of the floor 3.8 mm apart in a streamwise direction. All results are presented in a streamwise co-ordinate system, x, which has its origin at the inviscid shock reflection point. Boundary-layer pitot profiles were obtained using a flat-head pitot tube attached to a traverse mechanism. Total pressure was recorded using a pitot tube in the settling chamber.

Experimental Accuracy

Surface and pitot pressures were measured with fast-response pressure transducers, and the experimental error of these measurements is of the order of $\pm 1\%$ of the local value. The accuracy of the traverse gear used in the determination of boundary-layer profiles was better than 0.1 mm (1% of δ). However, when velocity profiles are evaluated from pitot pressure measurements in compressible flow, a number of assumptions are commonly made and, particularly near the surface, probe interference effects are likely to introduce uncertainties in the final data. Although it is not generally possible to quantify these errors, it is thought that velocity information is likely to suffer from uncertainties of the order of $\pm 5\%$ in the outer regions and $\pm 10\%$ in the inner regions ($y < 1$ mm) of the boundary layers.

Streamwise distance is measured relative to the inviscid shock impingement location; the determination of which (from the schlieren photographs) in itself is subject to uncertainties. The error in streamwise location is, therefore, of the order of ± 1 mm.

Data are also presented where streamwise location is scaled by upstream boundary-layer displacement thickness. These data are subject to a combination of uncertainties (such as the determination of displacement thickness from boundary-layer profiles). An analysis of boundary-layer displacement thickness measurements suggests that the maximum error is of the order of 0.2 mm on rough surfaces. For the larger roughnesses (P400 and P150) this is equivalent to 3–6% of δ^*, although the error incurred for the small roughness experiments (P1200) can be as much as 9% of δ^*. Therefore, the total uncertainty in the determination of scaled distance from the inviscid shock location can be as much as 20% for the smallest roughness (P1200) and small distances from the shock ($x/\delta^* \leq 1$). For most data points, however, this error is of the order of 5%.

The oblique shock wave also interacts with the boundary layers growing along the side walls of the working section. In all cases, this interaction was not strong enough to cause separation. Surface oil-flow visualization was performed to examine the floor interaction. This indicated that the region of two dimensionality extended for more than 50% of the span of the working section in all cases.

Results and Discussion

Before studying the interaction itself, boundary-layer velocity profiles were obtained at $x = 0$ for a flow without an incident shock wave, that is, no wedge present. Figure 5 shows the boundary-layer velocity profiles for the smooth wall and all roughness types, where roughness extended throughout the working section (case 7 in Fig. 4). It can be seen that increasing roughness results in thickened boundary layers and less full profiles. The incompressible shape factors ranged from $H_I = 1.30$ (smooth wall) to $H_I = 1.50$ (P150).

Figure 6 shows a comparison of schlieren pictures obtained for an interaction on a smooth surface and on the wall fitted with the largest roughness. It can be seen that the rough wall boundary layer is significantly thicker and that the rough wall interaction occupies a much larger streamwise distance. However, apart from the length scale, there appears to be no fundamental difference in the nature of the interaction itself. The effect of surface roughness on the pressure distribution through the interaction is shown in Figs. 7 and 8. It can be seen that for both shock strengths surface roughness leads to a significant increase in upstream influence and interaction length. The largest roughness (P150) has the most severe effect, but even for the small roughness (P1200), the influence can be seen clearly. There is a small kink in the surface pressure distributions for P1200 at both shock strengths, which might suggest a small separation. However, this feature is independent of the shock strength and does not appear in the cases with larger roughness (which would be expected to be more likely to separate) and, therefore, it is thought that this

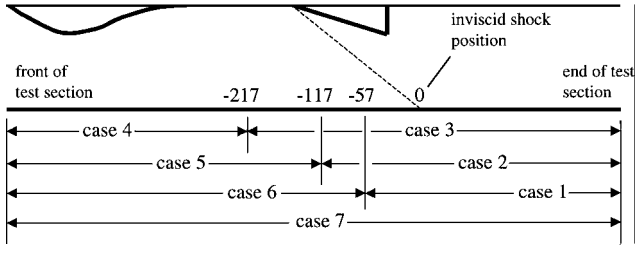

Fig. 4 Distribution of roughness; dimensions in millimeters.

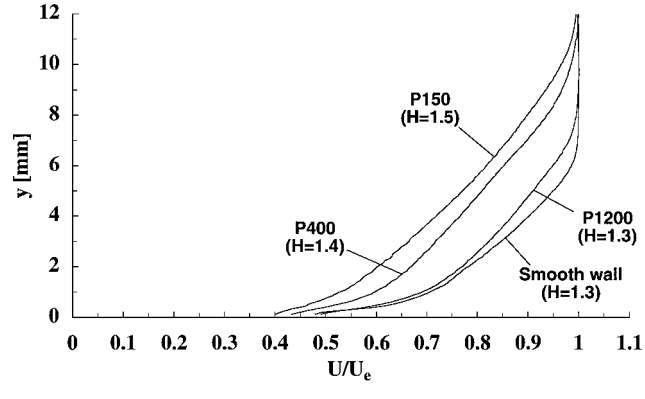

Fig. 5 Boundary-layer profiles upstream of interaction for various roughnesses.

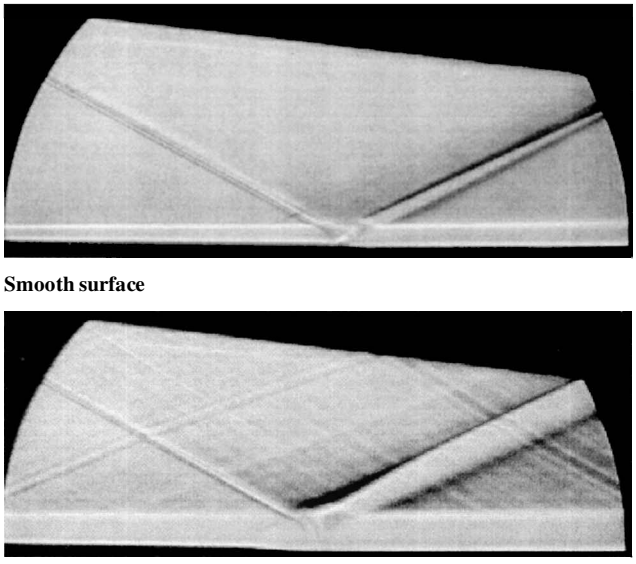

Smooth surface

Rough surface throughout (P150)

Fig. 6 Schlieren photographs of interaction.

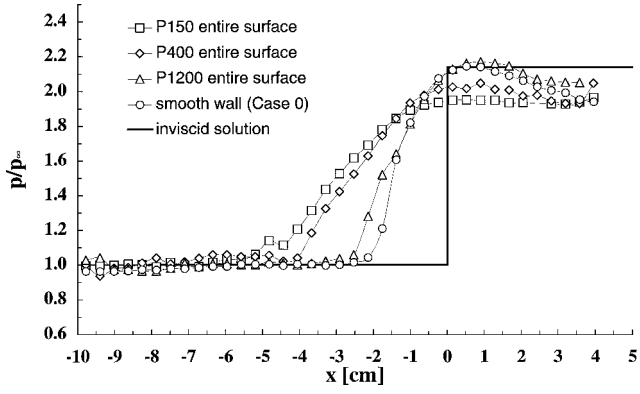

Fig. 7 Surface pressure distribution for 6-deg wedge angle.

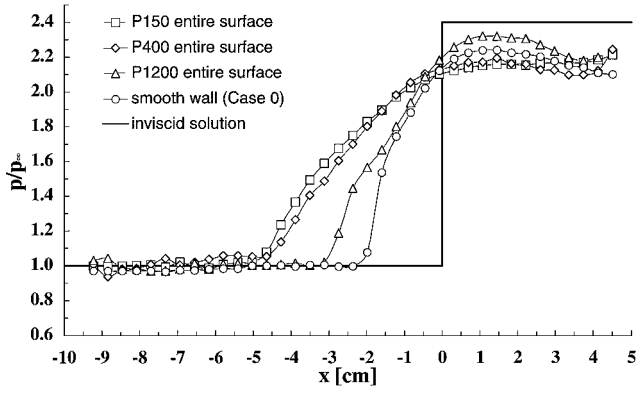

Fig. 8 Surface pressure distribution for 7-deg wedge angle.

kink is due to a flow nonuniformity at this location (caused by a wave reflected from the wind-tunnel ceiling originating from an insufficiently smoothed wall joint). Schlieren pictures and surface oil-flow visualizations did not suggest any significant separations.

As discussed earlier, previous research[7] suggests that upstream influence scales with boundary-layer thickness and shape factor. Because the experimental determination of boundary-layer thickness is difficult and prone to errors, it would be more useful to use the displacement thickness as the scaling parameter. In fact, because the ratio of boundary layer to displacement thickness is also a function of shape factor, the influence of H_I on upstream influence is almost completely contained in the change of δ^* alone. Furthermore, the theoretical investigation also suggests that displacement thickness may serve as a suitable scaling factor. This is demonstrated clearly in

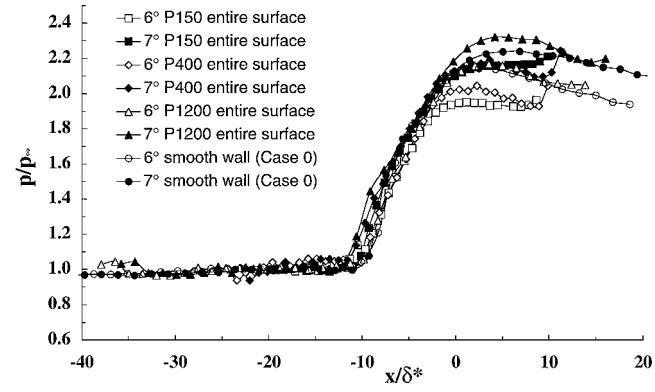

Fig. 9 Surface pressure distributions for both wedge angles (streamwise distance scaled with δ^*).

Fig. 9, which shows all previous surface pressure distributions after scaling the streamwise coordinate with displacement thickness. It can be seen that, within experimental accuracy, all curves collapse in the upstream part of the interaction regardless of wedge angle or roughness height.

This is somewhat surprising because previous research has often indicated a very strong change of interaction length with incoming boundary-layer shape factor. Although the range of shape factors here is somewhat limited, significant differences in interaction physics would still be expected. However, the interaction studied here is not thought to feature any separation, whereas those authors[1,2] who observed a strong influence of H_I studied mainly separated interactions. Therefore, it appears that shape factor is not a significant factor in attached interactions, whereas it has a large influence once separation occurs. This might also explain why some authors[4,8] have noted that differences in oncoming boundary-layer profile shape had relatively little influence on incipient separation.

However, a very close examination of Fig. 9 reveals that data recorded on a rough surface for the stronger shock setup (7-deg wedge angle) exhibit a slightly increased upstream influence. Because the data shown in Fig. 9 are subject to experimental uncertainties, first in the determination of the unscaled pressure distribution but more important in the accuracy of the evaluation of displacement thickness, this degree of variation in the perceived upstream influence is within experimental error. However, because it is only 7-deg wedge angle data that consistently show a slightly increased upstream influence, it might suggest that there is a degree of separation. This might indeed suggest that roughness does promote a somewhat earlier onset of separation. (The smooth wall data for 7 deg do not show increased upstream influence.)

Rough and Smooth Surface Mixed Cases

Figures 10–12 show the boundary-layer profiles obtained at the interaction location (but without the incident shock present) for all rough/smooth wall cases presented in Fig. 4. It can be seen that the presence of roughness can change the velocity profiles considerably, that the largest roughness height (P150) has the most significant effect, and that the smallest roughness (P1200) hardly changes the profiles. Nevertheless, all three roughness heights exhibit a similar pattern, with the mixed cases (cases 1–6) generating velocity profiles that lie in between the smooth wall (case 0) and the roughness-throughout (case 7) configurations. Furthermore, it can be seen that wherever a mostly smooth surface is followed by a short stretch of roughness (cases 1–3) the near-wall portion of the boundary layer is affected and that the velocity distribution in this portion is similar to that seen in the roughness-throughout configuration, whereas the outer portions of the velocity profiles remain similar to the undisturbed smooth wall profile.

On the other hand, in cases where a rough surface is followed by a short stretch of smooth wall (cases 4–6), the opposite effect can be observed. The near-wall boundary layer resembles a smooth wall profile, whereas the outer part of the boundary layer is similar to the fully rough velocity profile. In all cases, it is the extent of the rough/smooth surface immediately upstream of the measurement

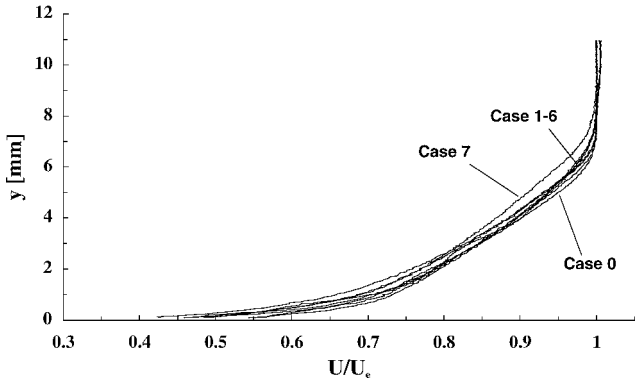

Fig. 10 Upstream boundary-layer profiles for various rough/smooth combinations: smallest roughness height (P1200).

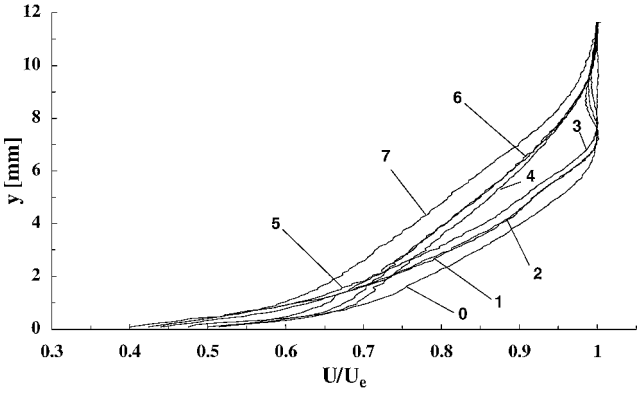

Fig. 11 Upstream boundary-layer profiles for various rough/smooth combinations: medium roughness height (P400).

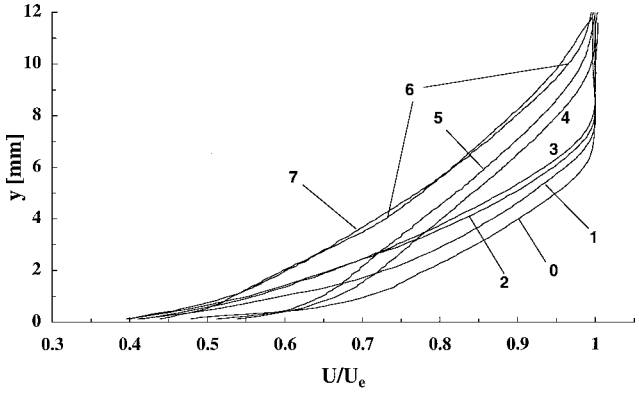

Fig. 12 Upstream boundary-layer profiles for various rough/smooth combinations: large roughness height (P150).

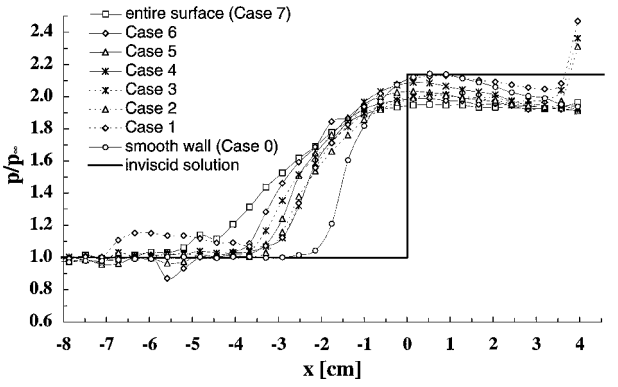

Fig. 13 Surface pressure distributions for large roughness (P150); 6-deg wedge angle.

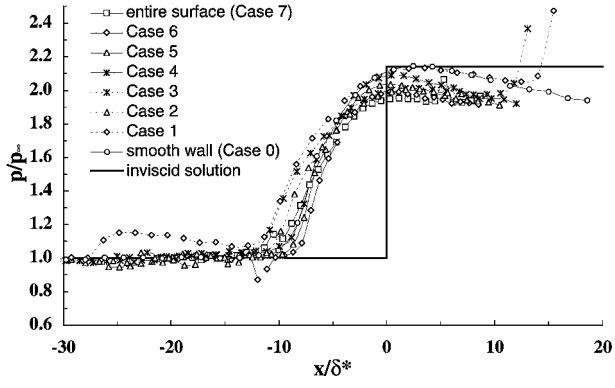

Fig. 14 Surface pressure distribution (scaled with δ^*), large roughness (P150); 6-deg wedge angle.

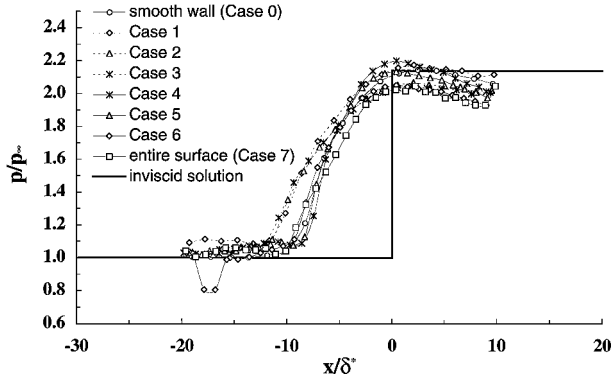

Fig. 15 Surface pressure distribution (scaled with δ^*), medium roughness (P400); 6-deg wedge angle.

location that determines how far into the boundary layer the effect of the surface property has extended.

Whereas the magnitude of the changes caused to the velocity profiles depend on the roughness height (the P150 roughness has a much more significant effect than the P1200 surface), the principal features of the mixed-case boundary-layer profiles are very similar for all three roughness heights. Depending on the combination of rough/smooth surface, it is, therefore, possible to study a rough wall interaction with an incoming boundary-layer profile that reflects mainly smooth wall behaviour and vice versa. Because of limitation in space and the earlier noted possibility of separation in some of the stronger shock experiments, only the 6-deg wedge angle data are presented here.

Figure 13 shows the surface pressure distribution for the largest roughness height (P150) and all combinations of smooth/rough wall. Note that the interaction length is strongly effected by the changes in surface properties and that all mixed cases (cases 1–6) lie in between the smooth (case 0) and completely rough (case 7) distributions. A similar behavior was observed for all other roughness heights. A number of high- and low-pressure regions upstream of the interaction can be seen in some of the traces of Fig. 13. These are due to waves generated by the sudden change in surface properties.

Figures 14–16 show the surface pressure distributions for the all combinations of smooth/rough surface and all three roughness heights, where the streamwise distance has been scaled with incoming boundary-layer displacement thickness. As for the data presented in Fig. 9, it can be seen that the upstream influence scaled with δ^* is very similar for all cases.

However, it can also be seen that some particular combinations of rough/smooth surface (cases 1–3) consistently exhibit an increased upstream influence regardless of roughness height (except for P1200, where only the case 3 data show this behavior). The data recorded for the smallest roughness height are likely to be subject to the largest inaccuracies, and it is, therefore, thought to be unwise to read too much into the results presented in Fig. 16. Therefore,

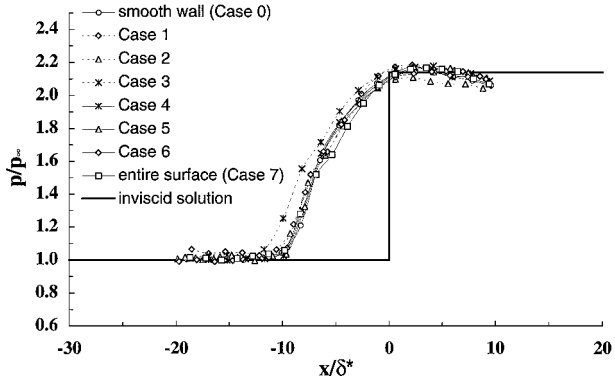

Fig. 16 Surface pressure distribution (scaled with δ^*), small roughness (P1200); 6-deg wedge angle.

it appears as if all configurations where a relatively short stretch of rough surface is located more or less in the interaction region itself feature slightly increased upstream influence, whereas configurations where the surface underneath the interaction is smooth (but there has been roughness farther upstream) show the same interaction behavior (when scaled with δ^*) as completely smooth/rough surfaces. This suggests, in accordance with the conclusions drawn from theory, that there is a residual effect of roughness beyond the changes to boundary-layer thickness and shape. However, this effect is small, and in none of the cases shown here (or for the stronger 7-deg wedge angle) has this been sufficient to cause any obvious signs of separation.

Conclusions

A nominally unseparated incipient shock-wave/turbulent boundary-layer interaction has been investigated on a variety of surfaces with step changes in surface roughness upstream of the interaction. Three roughness heights, ranging from hydraulically smooth to intermediate, were investigated.

In parallel, a theoretical investigation based on law of the wall/law of the wake and triple-deck theory ideas was conducted to study the effect of surface properties on an unseparated shock/turbulent boundary-layer interaction .

Where roughness was present throughout the working section, it was found that, even for roughness heights in the hydraulically smooth regime, incoming boundary layers were thicker and slightly less full than smooth wall profiles. Where step changes of surface roughness were present, boundary-layer profiles exhibited distinctly different characteristics in the near-wall and far-wall regions. It was found that a change in the surface properties first affected the near-wall boundary layer, while leaving the outer portion more or less undisturbed, and that it took considerable downstream distance before all of a boundary-layer profile was affected. This allowed the investigation of shock/boundary-layer interactions with mixed incoming velocity profiles, that is, with smooth wall characteristics in the near-wall region and rough wall characteristics in the outer region (after a transition from rough to smooth surface) and vice versa.

The theoretical investigation suggested that the main effect of surface roughness on a shock/turbulent boundary-layer interaction is captured by the change in incoming boundary-layer displacement thickness and that upstream interaction length should, therefore, scale with displacement thickness. Theory also identified a residual roughness effect but predicted this to be small. Experiments confirmed this prediction, and it was found that in all cases, including mixed surface properties, upstream distance of the interaction scaled well with incoming boundary-layer displacement thickness (to within 30%). If cases with a smooth to rough step change in surface properties are excluded, then all pressure distributions scaled with δ^* to within experimental accuracy.

It is suggested that mixed cases are subject to nonequilibrium effects in the boundary layer. Although the theoretical considerations appear to work well even in these cases, it is clear that, particularly for smooth to rough transitions, more thorough analysis is needed to capture these effects. A useful strategy would combine a triple-deck analysis in the SWBL interaction zone with a preceding two-layer-type theory of post roughness-jump relaxation.

Theoretical considerations also suggested an influence of surface roughness on incipient separation. Within the experimental investigation presented here, no consistent evidence of this has been found. This may be due to the limited height of roughness available.

In this program, experimental and theoretical research was carried out simultaneously, and each element of the study was used to influence and aid the other. It is thought that such a strategy is a very powerful tool for the investigation of complex interaction physics.

Acknowledgment

Part of this work was supported by NATO Grant CRG-951359.

References

[1]Disimile, P. J., and Scaggs, N. E., "Wedge-Induced Turbulent Boundary Layer Separation on a Roughened Surface at Mach 6.0," *Journal of Spacecraft and Rockets*, Vol. 28, No. 6, 1991, pp. 634–645.

[2]Holden, M. S., "Studies of Boundary Layer Transition and Surface Roughness Effects in Hypersonic Flow," U.S. Air Force Office of Scientific Research, AFOSR Rept. 6430-A-5, Washington, DC, Oct. 1983.

[3]Inger, G. R., "Supersonic Shock/Turbulent Boundary Layer Interaction on a Roughened Surface," *Journal of Propulsion and Power*, Vol. 12, No. 3, 1996, pp. 463–469.

[4]Babinsky, H., and Edwards, J. A., "Large-Scale Roughness Influence on Turbulent Hypersonic Boundary Layers Approaching Compression Corners," *Journal of Spacecraft and Rockets*, Vol. 34, No. 1, 1997, pp. 70–75.

[5]Inger, G. R., and Gendt, C., "Experimental Study of Transonic Shock/Turbulent Boundary Layer Interaction on a Roughened Surface," AIAA Paper 97-0065, Jan. 1997.

[6]Babinsky, H., Inger, G. R., and McConnell, A. D., "A Basic Experimental/Theoretical Study of Rough Wall Turbulent Shock/Boundary Layer Interaction," *Proceedings of the 22nd International Symposium on Shock Waves*, London, 1999, pp. 885–889.

[7]Déléry, J. M., "Shock Wave/Turbulent Boundary Layer Interaction and Its Control," *Progress in Aerospace Sciences*, Vol. 22, 1985, pp. 209–280.

[8]Squire, L. C., and Smith, M. J., "Interaction of a Shock Wave with a Turbulent Boundary Layer Disturbed by Injection," *Aeronautical Quarterly*, 1980, pp. 85–112.

[9]White, F. M., *Viscous Flow Theory*, 2nd ed., McGraw–Hill, New York, 1992, pp. 411–416.

[10]Inger, G. R., "Nonsymptotic Theory of Unseparated Turbulent Boundary Layer Interaction," *Numerical and Physical Aspects of Aerodynamic Flows*, edited by T. Cebeci, Springer-Verlag, New York, 1982, pp. 159–169.

[11]Lighthill, M. J., "On Boundary Layers and Upstream Influence; II. Supersonic Flow Without Separation," *Proceedings of the Royal Society of London, Series A: Mathematical and Physical Sciences*, Vol. 217, No. 1131, 1953, pp. 478–507.

[12]Kuehn, D. M., "Experimental Investigation of the Pressure Rise for Incipient Separation of Turbulent Boundary Layers in Two Dimensional Supersonic Flow," NASA Memo 1-21-59A, Feb. 1959.

[13]Gadd, G. E., Holder, D. W., and Regan, J. D., "An Experimental Investigation of the Interaction Between Shock Waves and Boundary Layers," *Proceedings of the Royal Society of London, Series A: Mathematical and Physical Sciences*, Vol. 226, No. 1165, 1954, pp. 227–253.

M. Sichel
Associate Editor